International Journal of Engineering and Science Invention (IJESI)
ISSN (Online): 2319-6734, ISSN (Print): 2319-6726
www.ijesi.org ||Volume 14 Issue 2 February 2025 || PP 06-15

Geostress field inversion and stress characterization of the Pan 'er Coal Mine in Huainan, China

Wu Hao
(College of Civil Architecture, Anhui University of Science and Technology, CHINA)

ABSTRACT: *To thoroughly elucidate the distribution patterns of in-situ stress within the Pan 'er Coal Mine in Huainan, China, this study systematically compiles and extensively analyzes existing test data. Utilizing advanced modeling and numerical simulation techniques via SolidWorks, ANSYS, SPSS, and FLAC3D, a precise three-dimensional spatial representation of the deep in-situ stress distribution within the mine is constructed. This comprehensive analysis unveils the intricate stress distribution characteristics of the in-situ stress field at the Pan 'er Coal Mine, thereby providing a robust scientific foundation for enhancing the safety and efficiency of coal resource extraction methodologies.*

KEYWORDS: *FLAC3D； Ground stress inversion ； Paner Coal Mine ； Regression analysis*

Date of Submission: 20-01-2025 Date of Acceptance: 05-02-2025

I. INTRODUCTION

In the domain of coal mining, in-situ stress is intrinsically linked to the safety and sustainability of resource extraction. It serves as the foundation for roadway design, the formulation of coal and gas outburst risk mitigation strategies, and the optimization of roadway and chamber support structures. A precise understanding of the distribution patterns and dynamic fluctuations of ground stress holds immense value in mitigating geological hazards, enhancing the safety of mining operations, and optimizing resource recovery efficiency.

Currently, the significance of in-situ stress testing and research is becoming increasingly apparent. For instance, drawing on geological structural exploration and measured in-situ stress data from a mine in Ningxia, Ren Huiliang et al. employed MIDAS to analyze the impact of the composite fault-fold structure on the distribution patterns and characteristics of in-situ stress. The results reveal that stress concentration and reduction zones, encompassing the maximum principal stress, minimum principal stress, and vertical stress, emerge on both sides of the fault's termination. These zones exhibit central symmetry about the geometric center of the fault section at both ends [1]. Taking a highway tunnel project in Honghe Prefecture, Yunnan Province, as a case study, Chen Shuang et al. conducted an analysis of the initial in-situ stress field in the tunnel site selection area, and subsequently examined the impact of faults and fracture zones on the distribution of in-situ stress. The results indicate that the stress is greatest along the horizontal vertical axis of the tunnel, with a decrease in stress observed within the fault zones. At the boundaries of the fault zones, stress increases, thereby elevating the likelihood of rock bursts [2]. Furthermore, focusing on the Yuchuan region, Zhang et al. developed a finite element simulation model leveraging an extensive dataset of seismic and rock mechanics information. This approach significantly enhanced the accuracy of simulating the in-situ stress field and elucidated the coupling relationship between in-situ stress, formation strain, and formation pressure. The findings reveal that the distribution of ground pressure is profoundly influenced by faults, structural orientations, and the physical properties of the rocks. Concentrated areas of ground stress are predominantly found in synclines and deeply buried strata [3].

At present, while Pan 'er Coal Mine in Huainan has conducted relevant in-situ stress testing, the scope is primarily limited to a single working face. Due to factors such as local structural influences, adjacent goafs, and other variables, the in-situ stress data obtained mainly reflects conditions in a localized area. As a result, the test outcomes are only applicable to guiding production activities specific to that working face and may not fully represent the broader in-situ stress situation throughout the entire mine [4]. Therefore, to comprehensively understand the distribution pattern of in-situ stress in Pan 'er Coal Mine, this study systematically organizes and thoroughly analyzes the existing test data. Using advanced simulation tools such as SolidWorks, ANSYS, SPSS, and FLAC3D, numerical simulations are conducted to precisely capture the three-dimensional spatial distribution characteristics of deep in-situ stress in the mine. This approach aims to fully uncover the stress distribution patterns within the in-situ stress field of Pan 'er Coal Mine and provide a scientific foundation for improving the safety and efficiency of coal resource mining technologies.

II. TEST METHODS

2.1 Establishment of numerical simulation model

2.1.1 Generalization of geological conditions

Pan 'er Coal Mine is located in Nihe Town, Panji District, in the northern region of Huainan City, Anhui Province, China. Based on the spatial extent of the coal mine and the strategic placement of in-situ stress measurement points, an area of 3,500 meters in length, 2,500 meters in width, and 1,200 meters in depth has been selected for the simulation and inversion analysis.

The geological formation of Pan 'er Coal Mine is intricately complex, characterized by multiple lithologic interactions with thin layers, numerous stratigraphic units, and parallel layering. Due to these complexities, an equivalent model and corresponding parameters have been employed, as opposed to a more detailed representation [5]. The inversion area has been simplified into six distinct layers, with the specific rock property parameters outlined in Table 1. In parallel, drawing upon the research methodologies of Hou Junling [6] and Yu Dajun [7], the regional faults have been generalized. The F5, F252, F2, and F1 faults, which exert a significant influence on the ground stress distribution within the coal mine, have been retained for further analysis.

Table 1 Inversion of rock physical and mechanical parameters in the study area

Tier number	Lamination thickness（m）	Density（kg/m^3）	Bulk modulus（GPa）	Shear modulus（GPa）	Force of cohesion（MPa）	Angle of internal friction（°）	Tensile strength（MPa）
First floor	260	2000	1.45	6.67	13.60	41.99	5.19
Second floor	240	2600	1.87	9.10	14.04	41.05	6.64
Third floor	220	2580	2.27	11.10	17.09	43.04	6.71
Fourth floor	150	2620	2.00	9.75	18.23	42.90	6.55
Fifth floor	130	2640	3.00	11.30	18.57	35.42	6.73
Sixth floor	200	2650	1.91	8.32	18.66	38.23	7.03

2.1.2 Establishment of 3D geological model and grid model

In accordance with the actual geological features of the inversion area, SolidWorks has been utilized to simulate the stratigraphic fluctuations and fault distributions. A three-dimensional geological model, with dimensions of 3,500 meters in length, 2,500 meters in width, and 1,200 meters in height, has been constructed, as depicted in Fig.1. To ensure the model's computability in FLAC3D, the APDL module in ANSYS has been employed for meshing the model. A gradual grid refinement technique has been used for the discretization of the model. The minimum unit side length near the faults is set to 60 meters, while the side length of the units farther from the faults gradually increases. The total number of grids in the model amounts to 1,148,956, and the grid division is illustrated in Fig.2.

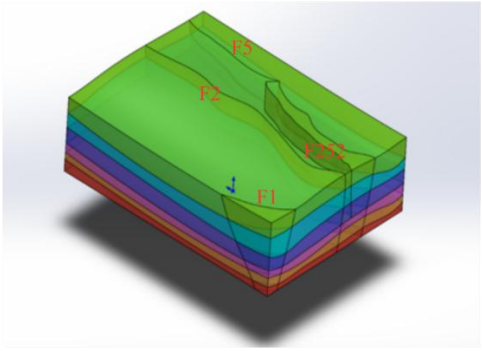

Fig.1 SolidWorks stratum model diagram

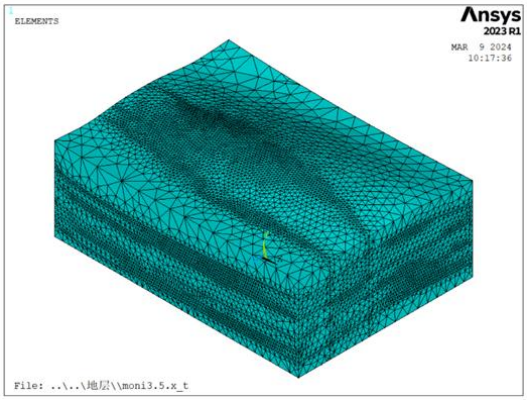

Fig.2 Three-dimensional grid diagram of ANSYS stratum model

2.2 Numerical simulation scheme

The model is discretized within APDL and subsequently imported into FLAC3D via the external conversion interface plug-in for simulation purposes. The resulting model is illustrated in Fig.3, where the X-axis denotes the east-west orientation, the Y-axis represents the north-south orientation, and the Z-axis signifies the vertical depth direction. The Mohr-Coulomb model is employed as the constitutive model for the simulation. The Ini command is utilized to define the initial stress conditions, while the Fix command is applied to establish the displacement boundary conditions for the model. Additionally, the base of the model is constrained with a condition of zero velocity.

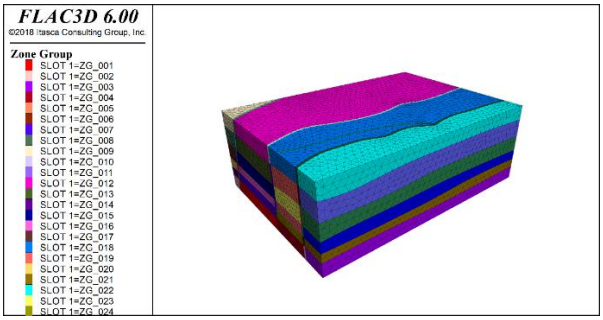

Fig.3 FLAC3D model

The initial in-situ stress field is influenced by various factors, including topography, lithology, and groundwater, with self-weight and geological tectonism being the primary contributors [8]. This study identifies six fundamental factors for the regression of the initial in-situ stress field in rock masses, as depicted in Fig.4. These factors are: 1) self-weight stress state; 2) vertical Y-axis horizontal compressive tectonic stress; 3) horizontal compressive tectonic stress parallel to the Y-axis; 4) vertical uniform shear deformation tectonic movement in the XZ plane; 5) vertical uniform shear deformation tectonic movement in the YZ plane; and 6) uniform shear deformation tectonic movement in the XY plane.

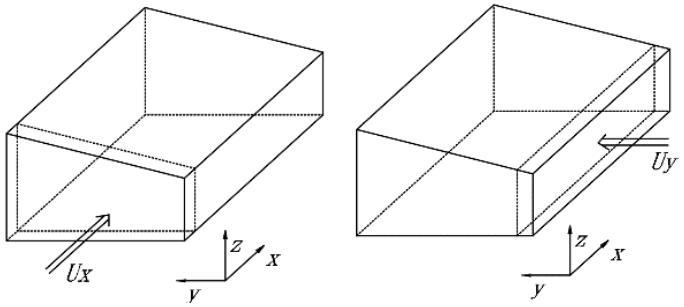

（a） （b）

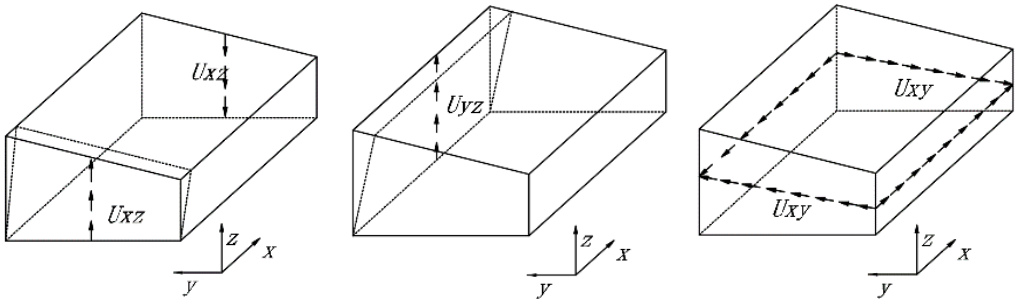

（c） （d） （e）

Fig. 4 Simplification diagram of unit tectonic motion

Thus, the simulation begins by inverting the six types of unit geological tectonic movements within FLAC3D, extracting the six stress components for each scenario, and developing a regression equation based on the measured values. Subsequently, SPSS is employed to determine the regression coefficients, yielding the ground stress regression equation for the formation model. This equation is then integrated into the FLAC3D calculation program to construct the initial ground stress field. Finally, a comprehensive simulation analysis of the geological model is conducted to derive the ground stress distribution pattern of the Pan'er Coal Mine.

III. RESULT ANALYSIS

3.1 Regression fitting analysis

SPSS software is employed to analyze the data from the six distinct working conditions, compute the regression coefficients, and derive the corresponding in-situ stress regression equation under homogeneous, isotropic conditions, as illustrated in Equation (1). Based on the data analysis outcomes, the Durbin-Watson statistic is 2.522, exceeding 2.5, which suggests a strong autocorrelation within this dataset, thereby affirming the validity of the regression model [9]. The coefficient of determination (R^2) and the adjusted R^2 of the regression are 0.941 and 0.871, respectively, signifying that over 87.1% of the variations in the initial in-situ stress are adequately explained by the model, reflecting a high degree of model fit. The results of the regression analysis are presented in Table 2 and Table 3.

$$\sigma=0.272\sigma_1+0.489\sigma_2+1.015\sigma_3+0.300\sigma_4+1.822\sigma_5+0.113\sigma_6 \quad (1)$$

Table 2 Goodness of fit evaluation of regression model and Durbin-Watson test results table

Model summary				
Model	R	R^2	Adjusted R^2	Durbin-Watson
1	0.970a	0.941	0.871	2.522

a. Prognosis variate：（Constant），VAR00006，VAR00005，VAR00003， VAR00001，VAR00002，VAR00004
b. Dependent variable：VAR00007

Table 3 Regression coefficient estimation and its significance test

Model		Non-normalized coefficients		Standardized coefficient	T	Significance
		B	Standard error	Beata		
1	VAR00001	0.272	0.067	0.637	4.033	0.010
	VAR00002	0.489	0.062	1.002	7.867	0.001
	VAR00003	1.015	0.221	0.530	4.596	0.006
	VAR00004	0.300	1.146	0.047	0.262	0.804
	VAR00005	1.822	1.513	0.192	1.205	0.282
	VAR00006	0.113	0.367	0.037	0.308	0.770

3.2 Stress analysis

Through the aforementioned procedures, the formulation of the initial in-situ stress field is successfully achieved, and the validity and precision of the inversion simulation are rigorously confirmed. A comprehensive multi-perspective analysis of the model inversion outcomes reveals the stress distribution pattern within the Pan'er Coal Mine.

(1) Vertical stress distribution

Upon meticulous examination of Fig.5(a), it becomes evident that the vertical stress component exhibits a negative value, with this magnitude increasing progressively as one moves downward along the vertical axis. Overall, the stress distribution demonstrates a relatively uniform pattern; however, a notable

concentration of stress is observed in the fault zone, indicating a pronounced localized anomaly. Fig.5(b), 5(c), and 5(d) illustrate the vertical stress profiles of the model at burial depths of 600 m, 800 m, and 900 m, respectively. A clear observation reveals that the vertical stress components are predominantly negative, with a general increase corresponding to the depth of burial. At the interface between the fault zone and the boundary, a marked discontinuity in stress is evident. In the shallower regions near the surface, stress is heavily influenced by geomorphological factors such as river channels and topographical elevations. However, as the burial depth increases, the influence of the surface topography on the in-situ stress diminishes progressively. It is evident that the stress distribution model unveiled by this inversion closely aligns with the actual geological conditions, demonstrating a high degree of congruence.

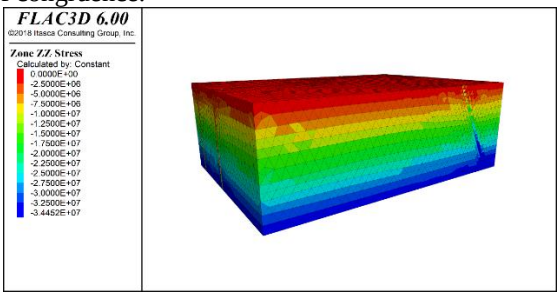

（a）stress cloud

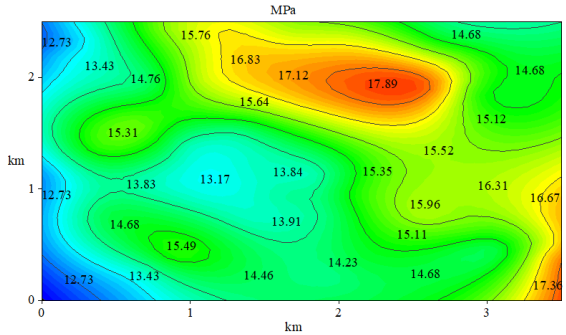

（b）stress isoline（*Z*=600m）

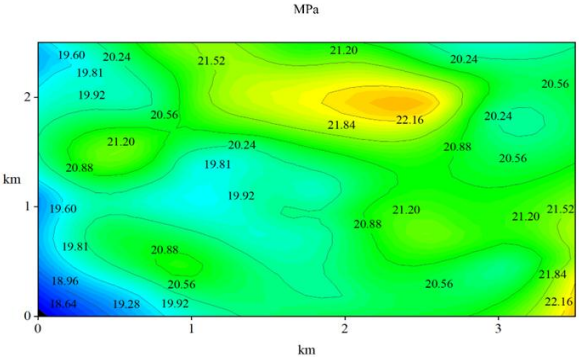

（c）stress isoline（*Z*=800m）

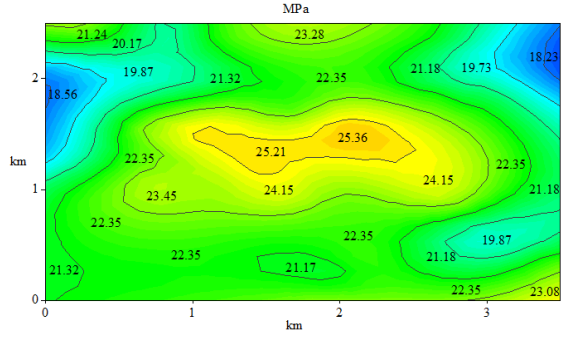

（d）stress isoline（*Z*=900m）

Fig.5 Vertical stress distribution profile cloud

(2) Maximum principal stress distribution

Fig.6 presents the cloud diagram of the maximum principal stress for the model. It is evident that the maximum principal stress intensifies with increasing depth. This escalation in stress underscores the intricate and heterogeneous geological conditions encountered in the deeper strata of the coal mine. The cloud diagram clearly reveals the phenomenon of stress concentration at the fault. As a vulnerable component of the geological structure, these faults are prone to stress accumulation under the influence of the surrounding stress field, leading to a marked increase in localized stress. The in-situ stress magnitude at Pan 'er Coal Mine is characterized by a high-stress state. Through stress analysis, it is evident that the principal stress distribution at this mine shows the vertical principal stress surpassing the maximum horizontal principal stress. Additionally, the predominant influence comes from the horizontal tectonic stress, which is a distinctive and typical feature of the site.

Fig.6(b), (c), and (d) illustrate the three-dimensional distribution cloud maps of the maximum principal stress for the 600 m, 800 m, and 900 m models, respectively. It is apparent that the rock strata are subjected to compressive stress. As the position moves closer to the center of the rock mass, the distribution of the maximum principal stress increases progressively, establishing a trend of decreasing stress from the core to the periphery. The stress exhibits a pronounced concentration at the corresponding fault zones, with the most apparent manifestation being the marked fluctuations observed in the three-dimensional stress distribution map.

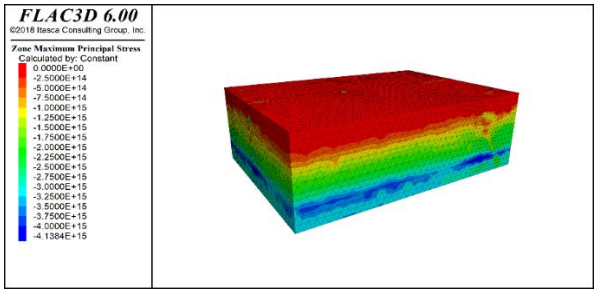

（a）Maximum principal stress cloud diagram

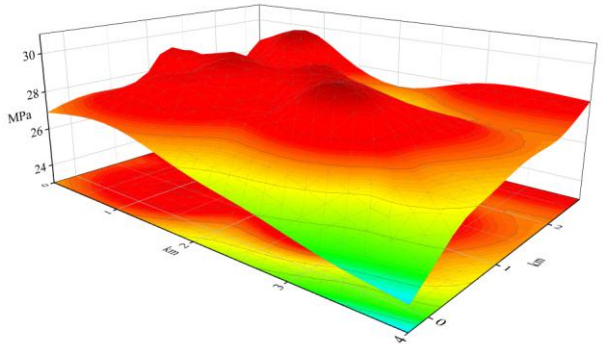

（b）Three-dimensional distribution map of maximum principal stress（*Z*=600m）

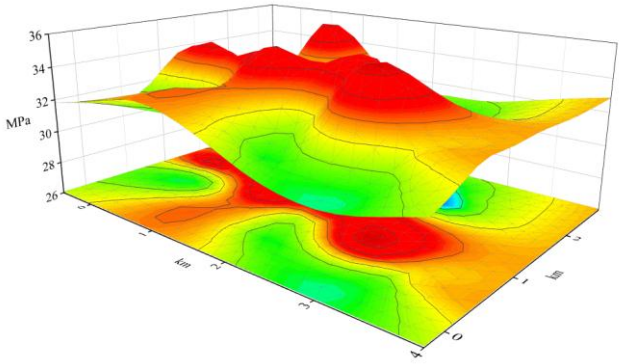

（c）Three-dimensional distribution map of maximum principal stress（*Z*=800m）

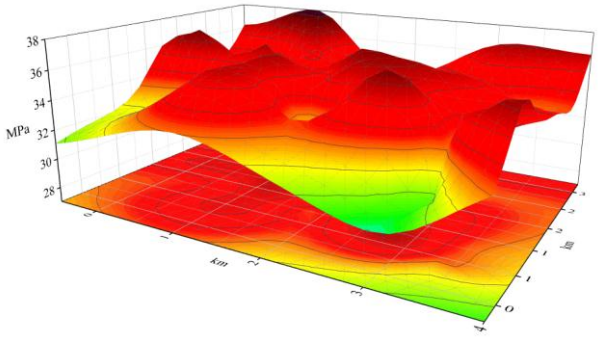

（d）Three-dimensional distribution map of maximum principal stress（Z=900m）
Fig.6 Maximum principal stress distribution cloud

(3) Distribution of minimum principal stress

Fig.7(a) presents the cloud diagram of the minimum principal stress for the model. As depth increases, the minimum principal stress within the rock mass exhibits a rising trend. This progression not only reflects the intrinsic behavior of stress variation with depth but also correlates closely with the stiffness of the rock strata, demonstrating a positive relationship. Moreover, the fault's influence on the minimum principal stress, as depicted in the figure, is notably pronounced. Particularly in proximity to the fault plane, there is a substantial reduction in the minimum principal stress, with stress concentration occurring at the fault tip.

Fig.7 (b), (c), and (d) present the three-dimensional distribution cloud maps of the minimum principal stress for the models at depths of 600 m, 800 m, and 900 m, respectively. It is evident that the rock strata are in a state of compression. As the position nears the core of the rock mass, the minimum principal stress distribution diminishes progressively, establishing a pattern of stress that gradually intensifies from the interior to the exterior. Furthermore, as a result of the directional and shear forces acting upon the model, the minimum principal stress is notably elevated on these applied surfaces, giving rise to a pronounced phenomenon of stress concentration.

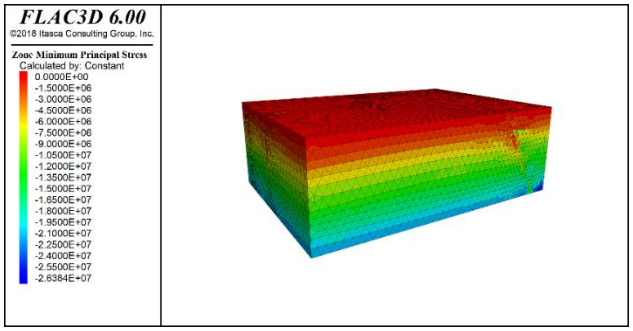

（a）Cloud diagram of minimum principal stress

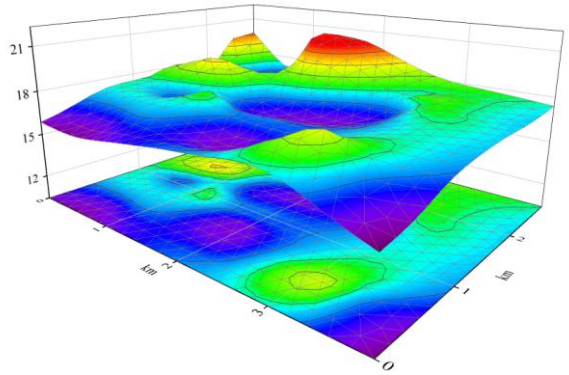

（b）Three-dimensional distribution map of minimum principal stress（*Z*=600m）

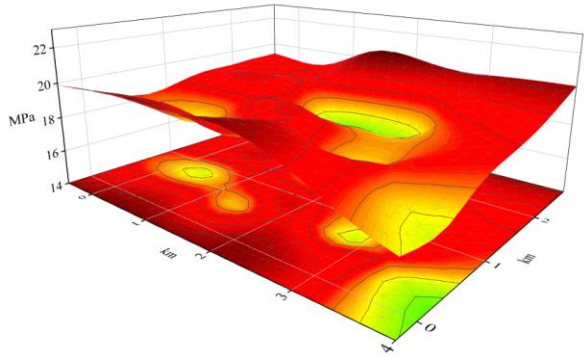

（c）Three-dimensional distribution map of minimum principal stress（*Z*=800m）

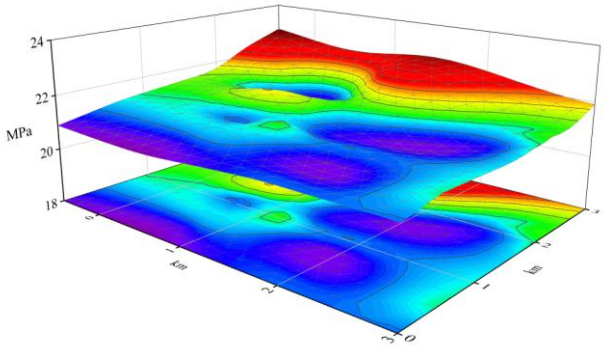

（d）Three-dimensional distribution map of minimum principal stress（*Z*=900m）

Fig.7 Cloud diagram of minimum principal stress distribution

3.3 Coal seam stress analysis

From Fig.8, the distribution of various stress types at the 700 m coal seam is evident. The direction and magnitude of the principal stresses at the coal seam exhibit a distinct pattern. The maximum principal stress aligns closely with the horizontal direction, while the minimum principal stress tends to align with the vertical direction. The magnitude of these principal stresses is influenced by multiple factors, including the depth of burial of the coal seam, the overburden weight, and the stiffness of the surrounding strata.

Simultaneously, in proximity to the fault, the stress distribution reveals distinct areas of concentration and reduction. The stress concentration at the fault tip induces an anomalous and complex stress state within the coal seam, while a defined region of stress reduction near the fault surface affects the stability and permeability of the coal seam. In conjunction with the overall distribution trend, as the depth of the coal seam increases, both vertical stress and tectonic stress exhibit a progressive rise. This escalation in stress may result in the accumulation of additional elastic strain energy within the coal, thereby amplifying the risk of coal and gas outbursts. At a burial depth of 700 meters, the maximum principal stress fluctuates between 25.37 MPa and 32.01 MPa, the intermediate principal stress ranges from 21.86 MPa to 25.51 MPa, and the minimum principal stress spans from 11.47 MPa to 21.46 MPa. Concurrently, the maximum lateral pressure coefficient oscillates from 1.024 MPa to 1.634 MPa, while the minimum lateral pressure coefficient varies between 0.545 MPa and 0.877 MPa.

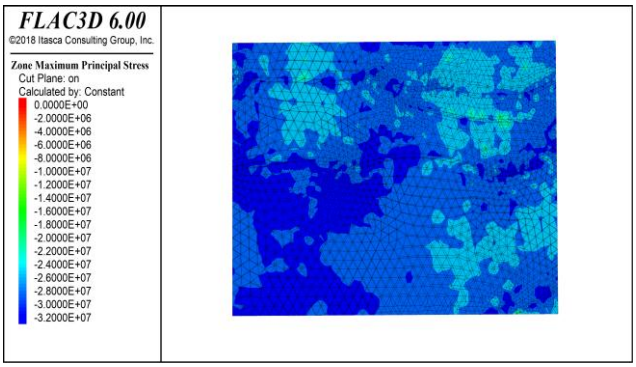

（a）Maximum principal stress cloud diagram（*Z*=700m）

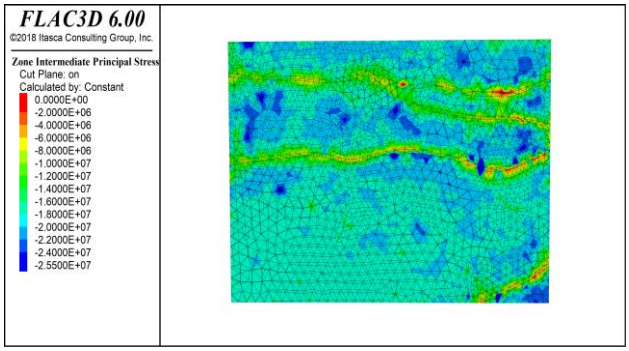

（b）Intermediate principal stress cloud diagram（*Z*=700m）

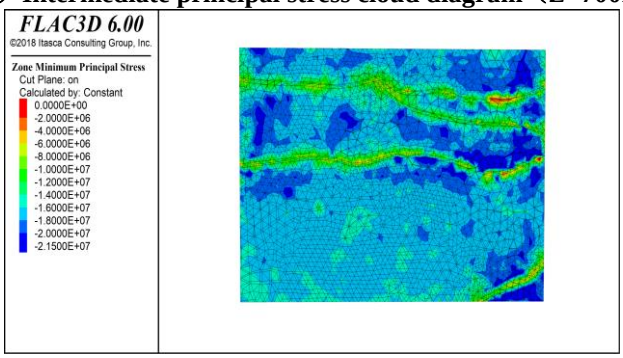

（c）Minimum principal stress cloud diagram（*Z*=700m）

Fig.8 Stress distribution cloud diagram at coal seam (Z = 700m)

3.4 Stress characteristic law

Through the inversion of in-situ stress and the acquired measurements, it is evident that the stress field within the Pan 'er Coal Mine is a tectonic stress regime influenced by fault structures and topographical variations. The stress state within the Pan 'er coal mine area remains relatively stable, with the overall distribution of the ground stress field characterized as follows:

The principal stress within the ground stress field is primarily the maximum horizontal principal stress, with an azimuth angle ranging from 85° to 129°, an inclination angle of less than 8°, and a nearly horizontal orientation. The intermediate principal stress exhibits an azimuth angle between 347° and 60°, an inclination angle exceeding 65°, and aligns closely with the vertical direction. The minimum principal stress, on the other hand, has an azimuth angle ranging from 175° to 219°, an inclination angle of less than 15°, and also follows a near-horizontal trajectory. Based on the inversion and measurement results of the ground stress, the intermediate stress closely approximates the vertical stress, and the ground stress field exhibits a stress relationship of $\sigma_1>\sigma_v>\sigma_3$. The horizontal stress surpasses the self-weight stress, signifying that the primary stress influencing the Pan 'er coal mine is tectonic in nature.

Consequently, the inversion results closely align with the observed conditions. They not only reflect the effects of stratigraphic variations and faulting but also underscore the importance of positioning the principal domain within the boundary conditions during inversion. This approach enhances the precision of the inversion process, yielding more reliable outcomes. At the periphery of the model, the accuracy of the inversion results is compromised due to the influence of multiple factors. This observation and subsequent analysis hold substantial importance for refining the inversion methodology and enhancing the precision of the resultant data.

IV. CONCLUSION

This paper conducts an in-depth study of the inversion simulation of the in-situ stress field at the Pan 'er Coal Mine in Huainan, China, yielding the following principal conclusions:

(1) A three-dimensional visualization model of the complex geological formations at Pan 'er Coal Mine is developed. The calculation domain’s three-dimensional model is constructed by integrating SolidWorks and ANSYS software, with post-processing analysis conducted using FLAC3D software. The spatial distribution of irregular, discontinuous, and dispersed geological data, derived from the coal mine's engineering geological surveys, is integrated into an intuitive, generalized three-dimensional geological model. This approach enhances and refines the construction methodology for in-situ stress inversion numerical models.

(2) The distribution characteristics of the in-situ stress field within the mining area are derived through the inversion of ground stress at Pan 'er Coal Mine. It is observed that the direction of the maximum principal

stress is predominantly horizontal. As the depth increases, the magnitude of the principal stress also escalates, with horizontal stress exhibiting a positive correlation to both burial depth and lithological composition. Notably, faults exert a pronounced influence on the stress field in their vicinity, leading to a reduction in the stress of the rock layers adjacent to the fault surface.

(3) The results of field measurements and inversion analysis indicate that the in-situ stress in Pan 'er Coal Mine is characterized by a state of high stress, predominantly governed by horizontal tectonic forces. The horizontal principal stress surpasses the vertical principal stress. Based on the inversion and measurement outcomes of ground stress, the intermediate stress approximates the vertical stress, and the stress field reveals a relationship where horizontal stress is greater than vertical stress. The horizontal stress exceeds the self-weight stress, suggesting that the primary contributor to the stress at Pan 'er Coal Mine is tectonic in nature.

REFERENCES

[1] Ren HuiLiang, Duan Dong, Chen Sishun.Influence of Composite Structure on the Distribution Characteristies of Geostress[J].Mining Research and Development,2019，39(6):58-62.

[2] Chen Shuang, Bai Genming, Xiao Chang， et al.Analysis of influence of fault structure on initial ground stress field of high ground stress tunnel[J].China Safety Science Journal，2023，33(2):146-151.

[3] Zhang Douzhong, Chen Kongquan, Tang Jiguang， et al.Prediction of formation pressure based on numerical simulation of in-situ stress field: a case study of the Longmaxi formation shale in the Nanchuan area， eastern Chongqing， China[J].Frontiers in Earth Science，2023，11.

[4] LI Qinsong.Comprehensive Early Warning Method of Gas Outburst Based on Microseismic Dynamic Response Law and Its Application[D].China University of Mining and Technology,2022.

[5] Wang Lixin, Li Hong, Liu Xiaomin, et al.Seismic exploration technologies of marine shale gas and their development directions in China[J].Acta Petrolei Sinica,2024,45(1):261-275.

[6] Hou Junlin.Inversion and Reconstruction Method of Deep Well Ground Stress Field in Huainan Mining District [D].Anhui University of Science and Technology,2014.

[7] Yu Dajun, Yang Zhangjie, Guo Yunhua, et al.Inversion method of initial geostress in coal mine field based on FLAC3D transverse isotropic model[J].Journal of China Coal Society,2020,45(10):3427-3434.

[8] Li Peng, Cai Meifeng, Guo Qifeng, et al.Research situations and development tendencies offault slip rockburst in coal mine[J].Journal of Harbin Institute of Technology,2018,50(3):1-17.

[9] Li Xiaoli.Study on Failure Mechanism of Buried Pipelines with Internal Corrosion Defects in Permafrost Regions[D].Northeast Petroleum University,2023.

[10] Kang Hongpu, Gao Fuqiang.Evolution of mining-induced stress and strata control in underground coal mines[J].Chinese Journal of Rock Mechanics and Engineering,2024,43(1):1-40.